AMERICAN SOCIETY FOR MICROBIOLOGY | mSphere®

RESEARCH ARTICLE
Therapeutics and Prevention

The Biofilm Inhibitor Carolacton Enters Gram-Negative Cells: Studies Using a TolC-Deficient Strain of *Escherichia coli*

Jannik Donner,[a] Michael Reck,[a] Boyke Bunk,[b,c] Michael Jarek,[d] Constantin Benjamin App,[a] Jan P. Meier-Kolthoff,[b,c] Jörg Overmann,[b,c] Rolf Müller,[e] Andreas Kirschning,[f] Irene Wagner-Döbler[a]

Department of Medical Microbiology, Group Microbial Communication, Helmholtz-Centre for Infection Research, Braunschweig, Germany[a]; Leibniz Institute DSMZ-German Collection of Microorganisms and Cell Cultures, Braunschweig, Germany[b]; German Centre for Infection Research (DZIF), Partner Site Hannover–Braunschweig, Braunschweig, Germany[c]; Genome Analytics, Helmholtz Centre for Infection Research, Braunschweig, Germany[d]; Department of Microbial Natural Products, Helmholtz Institute for Pharmaceutical Research Saarland (HIPS), Helmholtz Centre for Infection Research and Pharmaceutical Biotechnology, Saarland University, Saarbrücken, Germany[e]; Institute of Organic Chemistry and Center of Biomolecular Drug Research (BMWZ), Leibniz Universität Hannover, Hannover, Germany[f]

ABSTRACT The myxobacterial secondary metabolite carolacton inhibits growth of *Streptococcus pneumoniae* and kills biofilm cells of the caries- and endocarditis-associated pathogen *Streptococcus mutans* at nanomolar concentrations. Here, we studied the response to carolacton of an *Escherichia coli* strain that lacked the outer membrane protein TolC. Whole-genome sequencing of the laboratory *E. coli* strain TolC revealed the integration of an insertion element, IS*5*, at the *tolC* locus and a close phylogenetic relationship to the ancient *E. coli* K-12. We demonstrated via transcriptome sequencing (RNA-seq) and determination of MIC values that carolacton penetrates the phospholipid bilayer of the Gram-negative cell envelope and inhibits growth of *E. coli* TolC at similar concentrations as for streptococci. This inhibition is completely lost for a C-9 (*R*) epimer of carolacton, a derivative with an inverted stereocenter at carbon atom 9 [(*S*) → (*R*)] as the sole difference from the native molecule, which is also inactive in *S. pneumoniae* and *S. mutans*, suggesting a specific interaction of native carolacton with a conserved cellular target present in bacterial phyla as distantly related as *Firmicutes* and *Proteobacteria*. The efflux pump inhibitor (EPI) phenylalanine arginine β-naphthylamide (PAβN), which specifically inhibits AcrAB-TolC, renders *E. coli* susceptible to carolacton. Our data indicate that carolacton has potential for use in antimicrobial chemotherapy against Gram-negative bacteria, as a single drug or in combination with EPIs. Strain *E. coli* TolC has been deposited at the DSMZ; together with the associated RNA-seq data and MIC values, it can be used as a reference during future screenings for novel bioactive compounds.

IMPORTANCE The emergence of pathogens resistant against most or all of the antibiotics currently used in human therapy is a global threat, and therefore the search for antimicrobials with novel targets and modes of action is of utmost importance. The myxobacterial secondary metabolite carolacton had previously been shown to inhibit biofilm formation and growth of streptococci. Here, we investigated if carolacton could act against Gram-negative bacteria, which are difficult targets because of their double-layered cytoplasmic envelope. We found that the model organism *Escherichia coli* is susceptible to carolacton, similar to the Gram-positive *Streptococcus pneumoniae*, if its multidrug efflux system AcrAB-TolC is either inactivated genetically, by disruption of the *tolC* gene, or physiologically by coadministering an efflux pump inhibitor. A carolacton epimer that has a different steric configuration at car-

Received 22 August 2017 **Accepted** 26 August 2017 **Published** 27 September 2017

Citation Donner J, Reck M, Bunk B, Jarek M, App CB, Meier-Kolthoff JP, Overmann J, Müller R, Kirschning A, Wagner-Döbler I. 2017. The biofilm inhibitor carolacton enters Gram-negative cells: studies using a TolC-deficient strain of *Escherichia coli*. mSphere 2:e00375-17. https://doi.org/10.1128/mSphereDirect.00375-17.

Editor Patricia A. Bradford, Antimicrobial Development Specialists, LLC

Address correspondence to Jannik Donner, jannik.donner@helmholtz-hzi.de.

Solicited external reviewers: Bernd Kreikemeyer, University Medicine Rostock; Indranil Biswas, University of Kansas Medical Center; Rajeev Misra, Arizona State University.

This paper was submitted via the mSphereDirect™ pathway.

bon atom 9 is completely inactive, suggesting that carolacton may interact with the same molecular target in both Gram-positive and Gram-negative bacteria.

KEYWORDS Gram-negative bacteria, antimicrobial activity, antimicrobial agents, carolacton, drug efflux, drug resistance mechanisms, efflux pumps, gene sequencing, genome analysis

The identification of novel compounds for antimicrobial chemotherapy is becoming increasingly difficult (1). This is especially true for compounds targeting Gram-negative bacteria, for two main reasons: first, the second outer plasma membrane of Gram-negative organisms acts as a potent barrier and restricts the entry of hydrophilic extracellular substances, such as antibiotics, into the cell (2); second, the multidrug resistance (MDR) efflux systems present in many Gram-negative bacteria provide intrinsic resistance against antibiotics (3). The primary function of MDR efflux systems is the removal of toxins and bile acids from the cytoplasm, which is important for infectivity and virulence (4). MDR facilitated by extrusion of antibiotics has become a serious problem in the treatment of infections by, e.g., *Escherichia coli* (5), *Klebsiella pneumoniae* (6), *Pseudomonas aeruginosa* (7), and *Salmonella enterica* (8).

Proton-dependent tripartite envelope translocase systems (TETS) are widely distributed MDR efflux systems which have been studied extensively in *E. coli* and *P. aeruginosa*. TETS characteristically consist of an MDR pump, a membrane fusion protein (MFP), and an outer membrane factor (OMF) (9). In *E. coli*, MDR pumps of the resistance-nodulation-division (RND) family are key contributors to intrinsic antibiotic resistance (10). The genome of *E. coli* includes six genes for MDR pumps of the RND family (*acrB*, *acrF*, *yhiU*, *acrD*, *yegN*, and *yegO*) and seven genes for MFPs (*acrA*, *acrE*, *yhiV*, *yegM*, *emrA*, *emrK*, and *ybjY*) (11). As the third component of tripartite efflux systems, *E. coli* possesses four genes encoding OMF proteins, *tolC*, *mdtP*, *mdtQ*, and *cusC*, which are essential for a functional RND pump (e.g., AcrA-AcrB-TolC) (11). Among all OMF proteins of *E. coli*, TolC appears to be the major facilitator for extrusion of antibiotics and small molecules through the outer membrane (11, 12). In particular, the AcrAB-TolC tripartite efflux system is of great scientific interest, since it is constitutively expressed, has a broad substrate specificity, is found in a wide variety of clinically relevant Gram-negative pathogens (e.g., *P. aeruginosa*, *S. enterica*, and *Klebsiella* spp.), and contributes to MDR (4).

Therefore, efflux pump inhibitors (EPIs) can be important for the discovery of novel antibiotics (13), and they can be applied in combination with current antibiotics to overcome extrusion by MDR efflux systems (13, 14). Among them, the peptidomimetic EPI phenylalanine arginine β-naphthylamide (PAβN; MC-2077110) (15) was found to specifically block the AcrAB- and AcrEF-based MDR efflux systems in *E. coli*, which are both dependent on TolC as the OMF (16). On the other hand, bacterial strains with defects in MDR efflux systems are often used as sensitive indicators for antimicrobial activity (17). TolC mutants of *E. coli*, for example, are hypersensitive to 19 of 22 antibiotics tested (12).

The screening of libraries of natural secondary metabolites holds great promise for the discovery of novel antimicrobial compounds (18). During such screenings, the myxobacterial macrolide ketocarbonic acid carolacton was identified as a biofilm inhibitor (19, 20). Its activity against clinically relevant streptococci was later analyzed in great detail (20–24). The exact molecular target of carolacton remains unknown, but the complete loss of biological activity of a carolacton epimer at C-9 [(*S*) $\rightarrow$ (*R*)] (*epi*-carolacton) in *Streptococcus mutans* biofilms and planktonically growing *Streptococcus pneumoniae* cells (22, 24) suggests an interaction of carolacton with a conserved cellular target (24).

Carolacton is inactive against *E. coli* (MIC, $>$40 μg/ml), but strong growth inhibition was found when a laboratory *E. coli* strain recorded as lacking a functional copy of the OMF TolC (*E. coli* TolC) was treated with carolacton (MIC, 0.06 μg/ml) (19). These data suggested that carolacton might be able to pass through the Gram-negative cell

envelope and that the lack of sensitivity of wild-type *E. coli* to carolacton is due to export from the cell by TolC-mediated efflux. However, mutations in TolC can have different effects on substrate export, and there have even been reports that a misassembled TolC protein may result in an open channel which allows influx of antibiotics into the cell, resulting in an increased sensitivity (25). The TolC-deficient strain used in our screenings has been propagated as a glycerol stock in laboratories since at least 1980 (B. Kunze, personal communication), and so far it has not been characterized genetically. Over a period of 37 years, massive genetic changes could have occurred (26). Moreover, although TolC-deficient strains are used by many laboratories, they were constructed with different methods and in different genetic backgrounds (25, 27, 28), making it hard to compare results. We here determined the genome sequence of *E. coli* TolC with high resolution by using a combination of PacBio and Illumina sequencing. With these methods, an insertion of a natural transposon at the *tolC* locus was identified, and genetic changes were recorded that had occurred in this strain in comparison to its closest relative, which was identified as *E. coli* K-12 MG1655 (NZ_CP014225.1). We determined MICs for *E. coli* K-12 MG1655 and *E. coli* TolC and deposited *E. coli* TolC with the DSMZ as a tool and reference for future studies. We then studied the influence of carolacton on *E. coli* TolC by using transcriptome sequencing (RNA-seq), the carolacton C-9 (*R*) epimer, and the EPI PAβN. The data clearly showed that carolacton easily penetrates the Gram-negative cell envelope. Once inside the cell, it inhibits *E. coli* at similar concentrations as for streptococci, suggesting that the molecular target of carolacton is highly conserved and might be highly similar even in distantly related bacterial phyla, such as *Firmicutes* and *Proteobacteria*. The export of carolacton from the cell can be overcome by blocking the AcrAB-TolC efflux complex with the EPI PAβN. This finding highlights the potential use of carolacton in combinatorial treatment with EPIs.

RESULTS

***E. coli* TolC is an ancient natural derivative of *E. coli* K-12 and is closely related to K-12 MG1655.** PacBio single-molecule real-time (SMRT) sequencing and Illumina MiSeq short-read sequencing were combined to obtain a high-quality genome sequence of *E. coli* TolC. By Illumina MiSeq sequencing, 2,623,454 reads were obtained, totaling ~656 Mb and resulting in ~138-fold genome coverage. The PacBio SMRT sequencing data set consisted of 74,571 reads with an N50 read length of 17,770 bp and was used for *de novo* genome assembly. For the correction of indel errors, Illumina reads were mapped onto the newly assembled genome.

The genome of *E. coli* TolC (CP018801.1) consists of a single chromosome that is 4,792,200 bp long and contains 4,469 coding sequences (CDS), 88 tRNAs, 22 rRNAs, and 104 noncoding RNAs (ncRNAs). It was compared to all 259 fully sequenced *E. coli* genomes available from the National Center for Biotechnology Information (NCBI) via *in silico* DNA-DNA hybridization (*is*DDH), with *is*DDH values calculated by using the tool GGDC 2.1 (29). *E. coli* TolC showed the highest *is*DDH values (all *is*DDH values $\geq$98.28%) to *E. coli* strains K-12 MG1655 (NZ_CP014225.1), ER1821R (NZ_CP016018.1), NCM3722 (NZ_CP011495.1), K-12 W3110 (NC_007779.1), and JW5437-1 (NZ_CP014348.1).

A nucleotide-based genome BLAST distance phylogeny (GBDP) tree with branch support values inferred from both the nucleotide and amino acid data is depicted in Fig. S1 of our supplementary data posted on figshare (https://doi.org/10.6084/m9.figshare.5395471). The average branch support of the nucleotide tree was 47.3%, and branch support for the amino acid tree was 37.6%. Target strain *E. coli* TolC was placed in a highly supported subtree containing 14 strains, most of them K-12 strains.

Figure 1 shows the nucleotide sequence identity of *E. coli* TolC in comparison to the five most similar *E. coli* strains, as reported in BLAST+. Most notably, *E. coli* TolC contains the bacteriophage λ and the fertility plasmid F integrated into its chromosome. Phage λ was located between genes *ybhB* and *ybhC* at positions 3,079,545 to 3,128,200 of the *E. coli* TolC chromosome, and the F plasmid was integrated into an insertion sequence element (IS*3C*) within the cryptic prophage DLP12 (positions

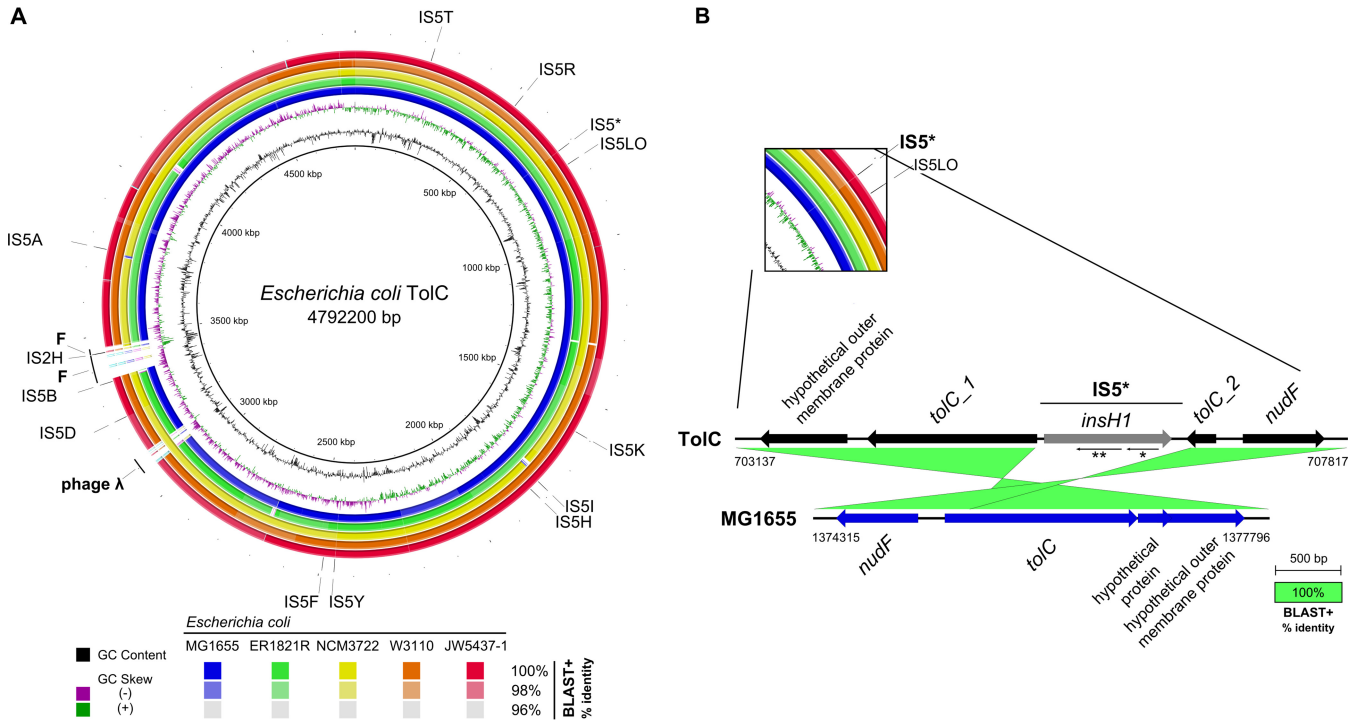

FIG 1 Whole-genome comparison of *E. coli* TolC to closely related strains and a schematic presentation of transposon-mediated disruption of the *tolC* CDS in *E. coli* TolC. (A) BLAST ring image generator (BRIG) (64) comparison of the *E. coli* TolC genome (innermost black ring) to the closely related genomes of *E. coli* strains K-12 MG1655, ER1821R, NCM3722, K-12 W3110, and JW5437-1 (the four outermost rings), shown in blue to red, respectively, as identified by *is*DDH (29). Shading of the four outermost rings is according to their respective percent nucleotide identity to the query sequence (*E. coli* TolC), determined by BLAST+. The second and third innermost rings show the GC skew (purple/green) and the GC content (black). IS*5* elements are numbered according to annotations for *E. coli* K-12 MG1655 (NC_000913.3). The location of the fertility plasmid on the chromosome of *E. coli* TolC is indicated by the letter F (on left side of diagram). (B) Close-up comparison of the *tolC* locus of *E. coli* TolC and its closest relative, *E. coli* K-12 MG1655, drawn by using Easyfig (66) The *tolC* locus (*tolC_1* and *tolC_2*) in *E. coli* TolC is interrupted by insertion of an IS*5* element (IS5*) that codes for the transposase *insH1* (*ins5A*). *ins5B* (**) and *ins5C* (*) are indicated by arrows in reverse orientation, underneath *insH1*. A BLAST+ comparison of the *tolC* locus for each of the two strains indicated 100% nucleotide identity.

3,368,702 to 3,467,447). This is in contrast to the most closely related *E. coli* strains, which encode neither the fertility plasmid nor phage λ, the only exception being NCM3722, which still carries phage λ (Fig. 1A). In comparison to MG1655, an *rph-1* mutation is absent in TolC, and the *rpoS* gene is present as the 33Am variant. Like other derivatives of *E. coli* K-12, strain *E. coli* TolC is also valine sensitive (*ilvG* deficient) (30). Similar to *E. coli* MG1655, an early deletion of two nucleotides (c.977_978delAT) that results in an Ile327-Glu substitution and subsequent insertion of a premature TGA translation termination site at position c.982_984 were found. As a common marker of all *E. coli* K-12 derivatives, *E. coli* TolC additionally carries an IS*5* insertion (IS*5*I) in the last gene of the O-antigen cluster encoding the rhamnosyltransferase WbbL (*rfb-50* mutation) (31). Although these strains are closely related, large structural rearrangements within their chromosomes were found (Fig. 2).

The *tolC* locus (*btd92_00696*) was inspected in detail, and the absence of a functional copy of the *tolC* gene was confirmed. The *E. coli* TolC strain carries a transposon insertion after base 1309 (c.1309_1310insIS*5**) of the *tolC* gene, and this causes a disruption of the CDS (Fig. 1B). Genes of the three additional OMF proteins in *E. coli* (*cusC*, *mdtQ*, and *mdtP*) were not affected (see Table S1 at https://doi.org/10.6084/m9.figshare.5395471). The transposon within *tolC* was identified as transposable element IS*5*, which contains three protein-coding genes: the transposase gene *insH1* (*ins5A*) and two genes (*ins5B* and *ins5C*) opposite *insH1* with unknown function (32, 33). Altogether, the *E. coli* TolC chromosome contained 12 insertions of IS*5* elements, of which only the one integrated into the *tolC* locus (IS*5**) disrupted a functional gene. Additionally, IS*5* insertions were also located within the sequences of cryptic prophages, e.g., the IS*5*Y element was inserted into the cryptic prophage Rac, interrupting *lomR*′. The *E. coli* TolC

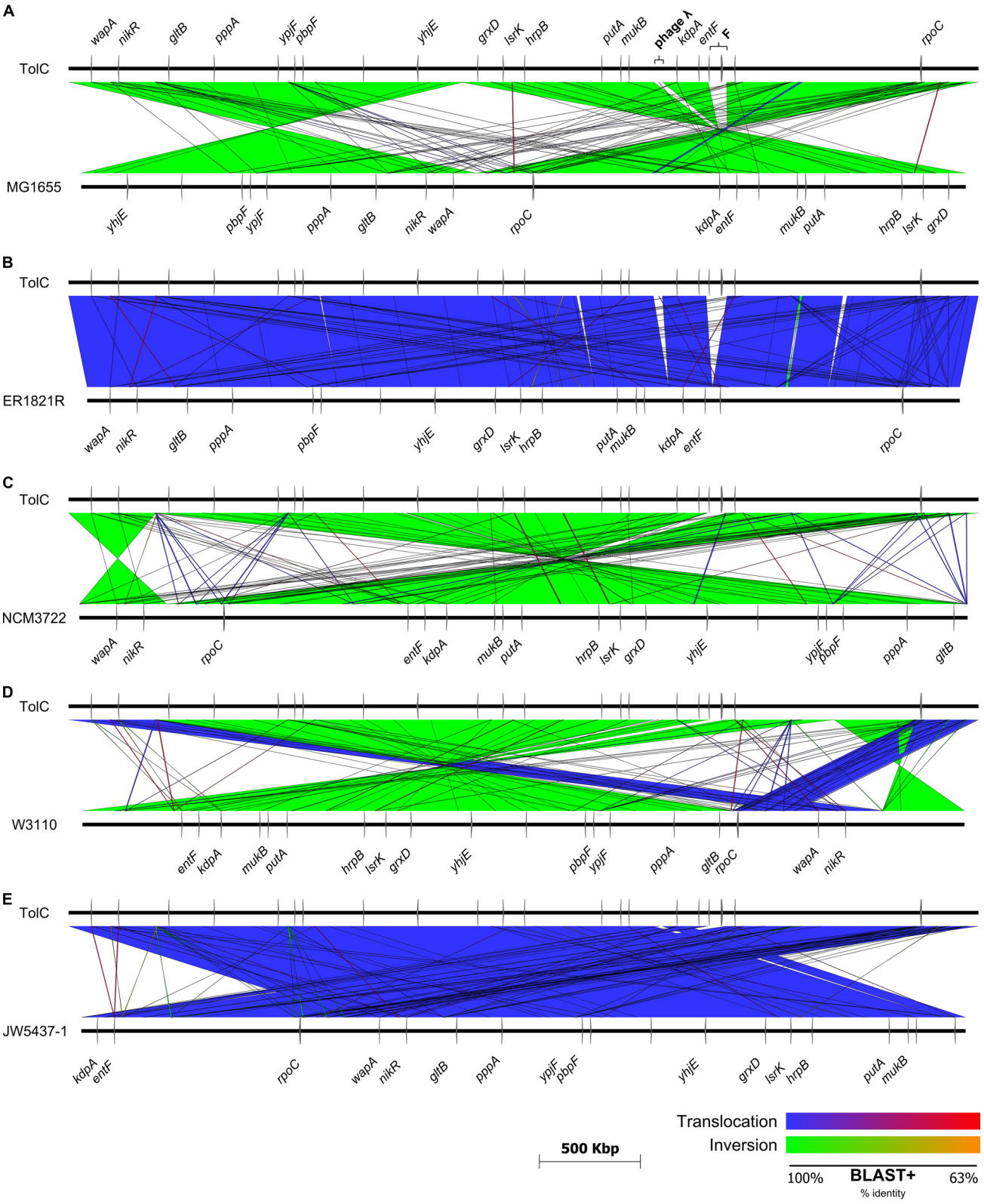

FIG 2 Genomic rearrangements of *E. coli* TolC in comparison with the most closely related strains. The complete genome of *E. coli* TolC was compared to the genomic sequences of *E. coli* K-12 MG1655 (A), *E. coli* ER1821R (B), *E. coli* NCM3722 (C), *E. coli* K-12 W3112 (D), and *E. coli* MG1655 JW5437-1 (E), and structural rearrangements were visualized using Easyfig (65). The relative locations of individual reference genes (in comparison to *E. coli tolC* in panel A) are indicated by gray arrows on the respective chromosomes (black horizontal lines). The nucleotide sequence identities, as determined using BLAST+, are indicated by different colored spectra: blue to red for translocations, and green to orange for inversions. Blue/green and red/orange indicate the highest (100%) and lowest (63%) detected sequence identities, respectively.

TABLE 1 MICs of antibiotics and carolacton against *E. coli* TolC and *E. coli* K-12 MG1655

Mechanism and/or antibiotic	Target	MIC (μg/ml)[a]		FC[b]
		E. coli K-12 MG1655	*E. coli* TolC	
Carolacton		>8	**0.125**	64
Carolacton with (40 μg/ml PAβN)		4	**≤0.03**	128
Protein biosynthesis				
Chloramphenicol	50S ribosomal subunit	8	**1**	8
Erythromycin	50S ribosomal subunit	>64	**2**	32
Gentamicin	30S ribosomal subunit	4	2	2
Kanamycin	30S ribosomal subunit	8	4	2
Peptidoglycan biosynthesis				
Ampicillin	Penicillin-binding proteins	16	**4**	4
Cephalotin	Penicillin-binding proteins	16	8	2
Cefotaxime	Penicillin-binding proteins	0.0625	**0.015**	4
Penicillin G	Penicillin-binding proteins	>32	16	2
Vancomycin	D-Ala-D-Ala moieties of NAM/NAG[c] peptides	>256	>256	1
Phosphomycin	UDP-*N*-acetylglucosamine-3-enolpyruvyltransferase (MurA)	>32	**4**	8
Fatty acid biosynthesis				
Triclosan	Enoyl-acyl carrier protein reductase (FabI)	0.125	**≤0.0078**	16
Cerulenin	β-keto-acyl-ACP synthase (FabB)	>32	**4**	8
RNA biosynthesis				
Corallopyronin A	RNA polymerase	>32	**2**	16
Rifampin	RNA polymerase	16	8	2
Sorangicin	RNA polymerase	16	16	1
Cell division				
Novobiocin	DNA gyrase	>16	**1**	16
Ciprofloxacin	DNA gyrase	0.015	**0.0039**	4
Folate biosynthesis				
Trimethoprim	Dihydrofolate reductase (FolA)	0.5	**0.063**	8
Sulfamethoxazole	Dihydropteroate synthase (FolP)	128	64	2

[a]Boldface values indicate that MICs for the MG1655 control strain differed by ≥4-fold.
[b]The FC increase in susceptibility of *E. coli* TolC relative to *E. coli* MG1655 susceptibility.
[c]NAM, *N*-acetylmuramic acid; NAG, *N*-acetylglucosamine.

strain described here was deposited at the Leibniz Institute DSMZ German Collection of Microorganisms and Cell Cultures (Braunschweig, Germany) and assigned strain number DSM 104619.

Role of TolC for MICs of carolacton and different classes of antibiotics. To evaluate the effect of TolC inactivation on antibiotic susceptibility of *E. coli*, the MICs of selected antibiotics against *E. coli* MG1655 and *E. coli* TolC were determined (Table 1). We included two RNA polymerase inhibitors, corallopyronin A and sorangicin, previously isolated from myxobacteria at our institution (34, 35).

E. coli TolC was at least 64 times more sensitive to carolacton than *E. coli* MG1655. The MIC of carolacton against *E. coli* TolC was in the same range as that reported by Jansen et al. (19). For *S. pneumoniae* TIGR4, the MIC of carolacton was determined to be 0.06 μg/ml (24), similar to the value reported for *E. coli* TolC. In comparison to *E. coli* MG1655, *E. coli* TolC showed a strong increase in sensitivity (≥4-fold) to antibiotics from all functional groups. The determined MICs were in the same range as those reported previously for *E. coli* W3110 and its *tolC* null mutant (11), indicating that the presence of the F plasmid and phage λ do not affect antibiotic susceptibility. Rifampin and vancomycin are not substrates of the pump; thus, *E. coli* TolC is not expected to be hypersensitive to these compounds, which was confirmed. The data indicated that carolacton penetrates the two membranes of the Gram-negative cell envelope and that its intracellular inhibitory effect is comparable to that of Gram-positive cells.

Transcriptional response of *E. coli* TolC to carolacton. We analyzed the transcriptome of carolacton-treated cultures of *E. coli* TolC in comparison to untreated cultures during the first 30 min of growth.

In total, 4,730 transcripts of *E. coli* TolC were investigated using Rockhopper (see Data Set S1 in the supplemental material). At 30 min after addition of carolacton, 71 transcripts showed a strong differential abundance ($\log_2$ fold change [FC] of $\geq \pm 2$), corresponding to 1.6% of all open reading frames of *E. coli* TolC (Data Set S2). At this time point, *E. coli* TolC grows at the same rate with or without carolacton (see below). The data therefore provide additional proof that carolacton immediately enters the Gram-negative cell. At a $\log_2$ FC of $\geq \pm 0.8$, approximately 29% of all genes were differentially abundant, comparable to the degree of differential transcript abundance in *S. mutans* (31.3%) and *S. pneumoniae* (22.8%) in the presence of carolacton when we used an identical cutoff (21, 24). The most strongly differentially abundant transcripts encoded components for flagellar assembly, heat shock and cold shock proteins, and chaperones (Fig. 3). Transcription of the alternative sigma factor F (σ^{28}) was upregulated ~7.4-fold ($\log_2$ FC, 2.88), and the putative helix-turn-helix (HTH)-type transcriptional regulator RhmR was downregulated. Moreover, precursors of the outer membrane pore proteins NmpC (*btd92_03329*) and PhoE (*btd92_03746*) were upregulated. Interestingly, all 7 StyR-44 family small noncoding RNAs encoded in the genome were strongly ($\log_2$ FC, ≥ 6.5) upregulated after only 5 min of growth with carolacton. The data showed that interaction of *E. coli* TolC with carolacton triggers global transcriptional adaptations already after 5 min, suggesting a molecular target in a central metabolic pathway.

Stereospecificity of carolacton activity and inhibition of efflux. Subsequently, the differences in carolacton susceptibility between *E. coli* TolC and *E. coli* MG1655 were investigated in detail over all growth phases. *E. coli* MG1655 with and without carolacton and TolC without carolacton grew similarly and reached their maximal optical density at 600 nm (OD_{600}) of ~6 after 7 h (Fig. 4A). In the presence of carolacton (added at $t = 0$), growth was indistinguishable from the controls for 1 h. At this time point, growth of the carolacton-treated culture of the *E. coli* TolC strain was strongly inhibited, while all other strains entered the exponential growth phase. The carolacton-treated culture of the *E. coli* TolC strain grew linearly over the next 5 h to an OD_{600} of approximately 0.8, which did not increase much farther and reached a maximal OD_{600} of around 1 after 24 h. Complementation of *E. coli* TolC with a plasmid-borne copy of the OMF TolC was able to restore insensitivity to carolacton, confirming indeed the absence of TolC-mediated efflux of carolacton as the sole cause for sensitivity (Fig. 5).

epi-Carolacton is a carolacton epimer with an inversion of the stereocenter at C-9 from the native (*S*) to the (*R*) configuration. This carolacton derivative lacks biological activity in *S. pneumoniae* TIGR4 and *S. mutans* UA159 (22, 24). Here, we tested the inhibitory properties of *epi*-carolacton against *E. coli* TolC. Figure 4B shows that *epi*-carolacton had no influence on growth of *E. coli* TolC. Since *epi*-carolacton was dissolved in dimethyl sulfoxide (DMSO), we investigated its effect on growth as an additional control, but we did not detect any. The loss of growth inhibition of *epi*-carolacton shown here suggests that the molecular target of carolacton might not only be conserved in the genus *Streptococcus* but also in the phyla *Firmicutes* and *Proteobacteria*.

Antibiotics that are substrates of TolC have to be administered in high doses to overcome the intrinsic resistance mediated by efflux (13). Alternatively, they could be applied in combination with efflux pump inhibitors. Therefore, we investigated the influence of PAβN, a competitive inhibitor of AcrAB-TolC (16), on carolacton sensitivity in *E. coli*. Table 1 shows that the MIC of *E. coli* MG1655 toward carolacton was reduced from >8 μg/ml to 4 μg/ml when PAβN was coadministered at 40 μg/ml. Lower concentrations of PAβN had no effect on the MIC of carolacton. The susceptibility of the TolC mutant was also increased by PAβN. The MIC of *E. coli* against PAβN has been shown before to be strongly reduced in an efflux-deficient strain (Δ*acrAB*); moreover, PAβN can cause membrane destabilization as an unspecific side effect (16). Accord-

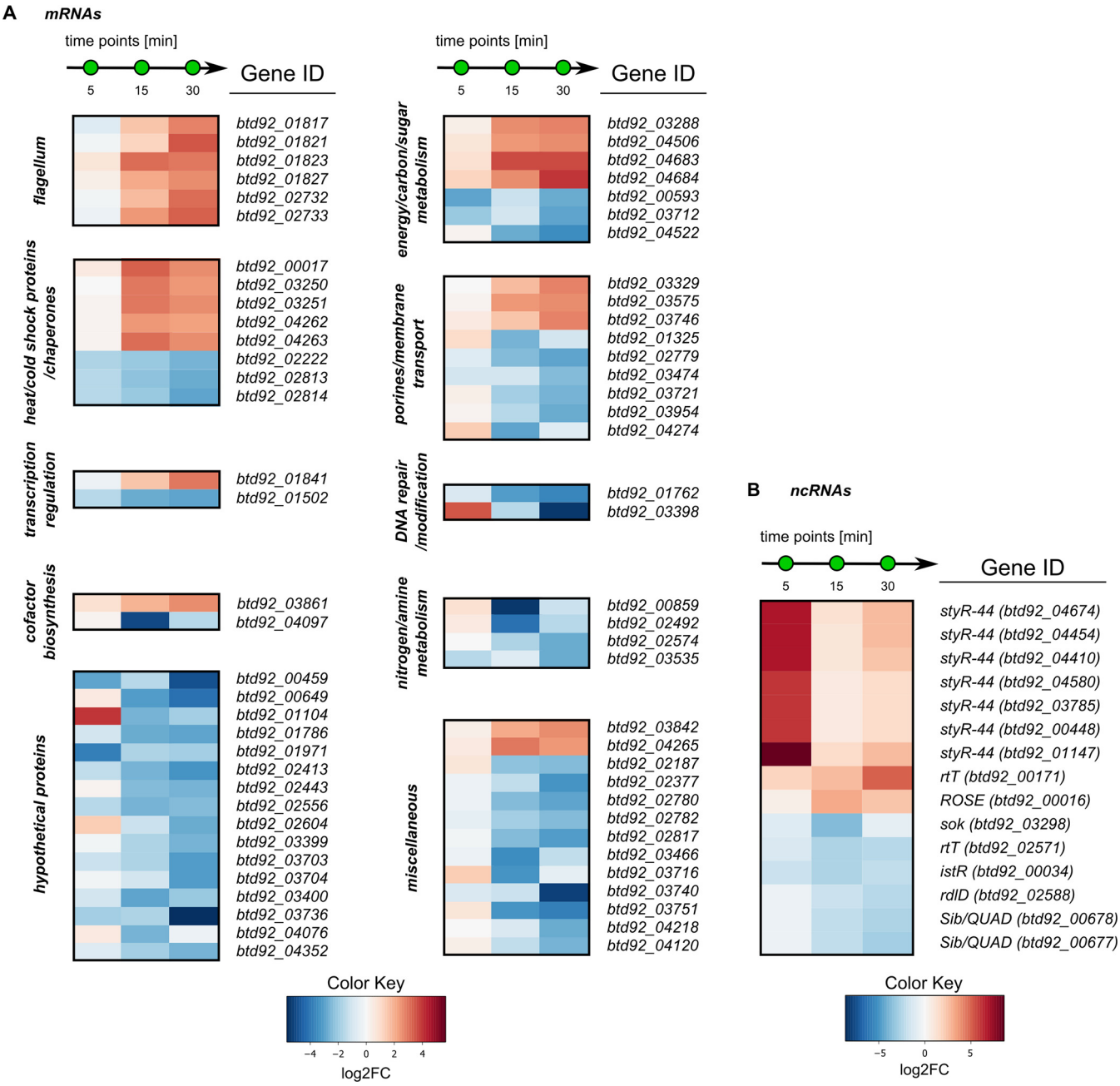

FIG 3 The most strongly differentially abundant transcripts in *E. coli* TolC during growth with carolacton (0.25 μg/ml). (A) Overview; (B) the most strongly differently regulated ncRNAs. The cutoff for differentially abundant transcripts was set at $\log_2$ FC of $\geq \pm 2$ for general transcripts and $\geq \pm 2.5$ for ncRNAs (FDR, ≤ 0.01), for at least one sample during the time course.

ingly, we observed a growth reduction of ~45% for the efflux-deficient *E. coli* TolC strain when grown with 40 μg/ml PAβN, but not for the wild-type (Fig. 5).

Finally, we investigated the role of PAβN (Fig. 6A) under the same conditions as those used for studying the effect of TolC deletion. The effect of PAβN on growth inhibition of *E. coli* MG1655 by carolacton was dependent on the concentration of PAβN used (Fig. 6B). At concentrations of 20 and 40 μg/ml PAβN, a maximal inhibition of 59% and 78%, respectively, was found, in comparison to a culture treated with only carolacton. The observations concerning MICs and a PAβN-mediated growth inhibition by carolacton were reproducible for the *tolC*-complemented *E. coli* TolC strain (Table 2 and Fig. 5, respectively). For comparison, inhibition of growth of *E. coli* TolC treated with

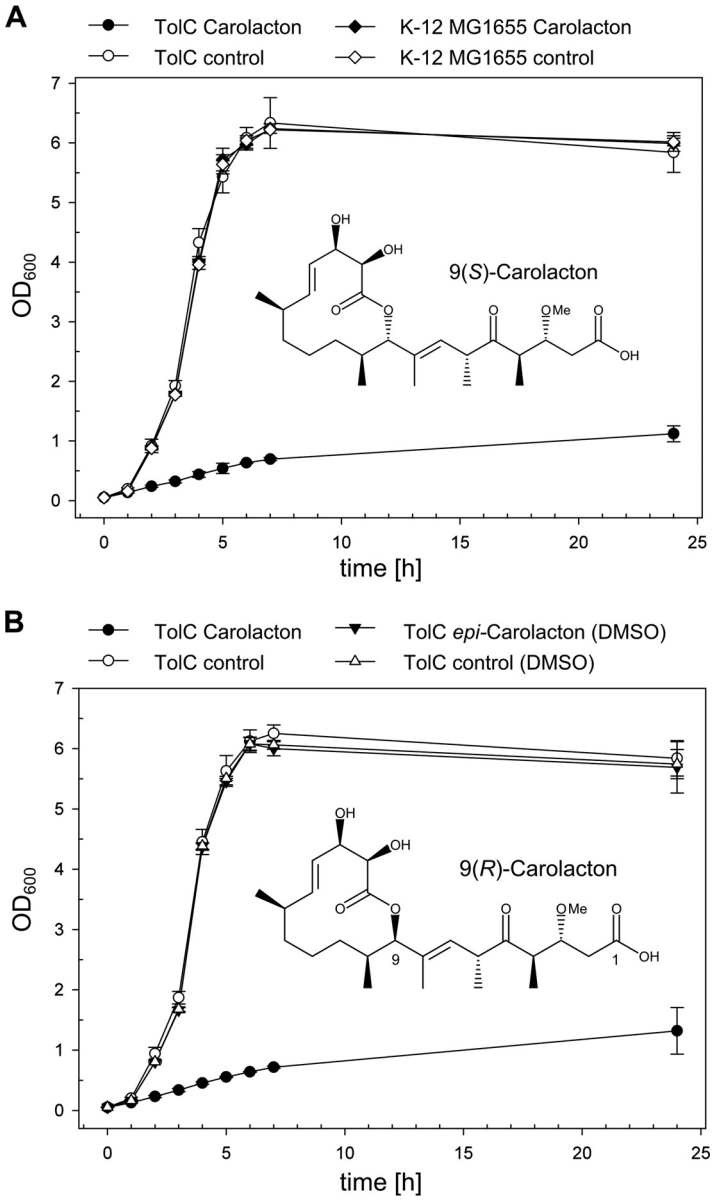

FIG 4 Growth inhibition of *E. coli* TolC and *E. coli* K-12 MG1655 by carolacton and sensitivity of *E. coli* TolC to *epi*-carolacton. (A) Chemical structure of native 9(*S*) carolacton and growth inhibition of *E. coli* TolC and *E. coli* K-12 MG1655 with 9(*S*) carolacton. (B) Structure of 9(*R*) carolacton (*epi*-carolacton) and inhibition activity against *E. coli* TolC treated with carolacton-methanol (circles) or in the presence of *epi*-carolacton and DMSO (triangles) for 24 h. Growth curves represent the mean (and standard deviation) results of three independent experiments, Carolacton was added at a final concentration of 0.25 μg/ml at $t = 0$ min.

carolacton is shown, which reached a maximum of 90% in comparison to the untreated culture (Fig. 6B). Thus, in *E. coli*, addition of 40 μg/ml PAβN, together with carolacton, causes a growth reduction similar to that with treatment with carolacton in a TolC-deficient strain.

The observed growth inhibition characteristics of carolacton- and PAβN-treated cultures of *E. coli* TolC and *E. coli* MG1655 were also reflected in drastic changes in the maximal doubling time (t_D) of cells during exponential growth (Table 3). The t_D of *E. coli* TolC after treatment with carolacton increased from 25 to >372 min (Fig. 4 and 7). A comparable decrease of the doubling time was also observed after coadministration of PAβN and carolacton to cultures of *E. coli* MG1655 (t_D, ~257 min), supporting the previous observation that PAβN treatment can facilitate a carolacton-dependent slow-

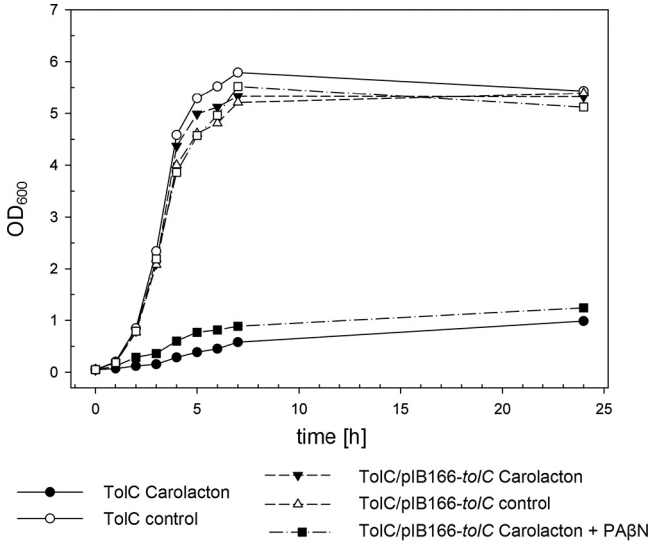

FIG 5 Complementation of the *E. coli* TolC strain with a plasmid-carried copy of *tolC*. For expression of a functional copy of TolC in *E. coli* TolC, the *tolC* gene and native regulatory sequences were PCR amplified from *E. coli* MG1655 and cloned into pIB166, and the resulting construct was transformed into *E. coli* TolC. *E. coli* TolC/pIB166-*tolC* was grown with 20 μg/ml chloramphenicol, and the AcrAB-TolC efflux pump inhibitor PAβN was applied at a final concentration of 40 μg/ml. The growth curves are representative of results for three biological replicates.

down of cell division and consequently growth inhibition of an otherwise-resistant strain.

DISCUSSION

Here we studied the role of TolC, a component of the major multidrug efflux system of *E. coli*, in its susceptibility to carolacton. To this end, we determined the genome

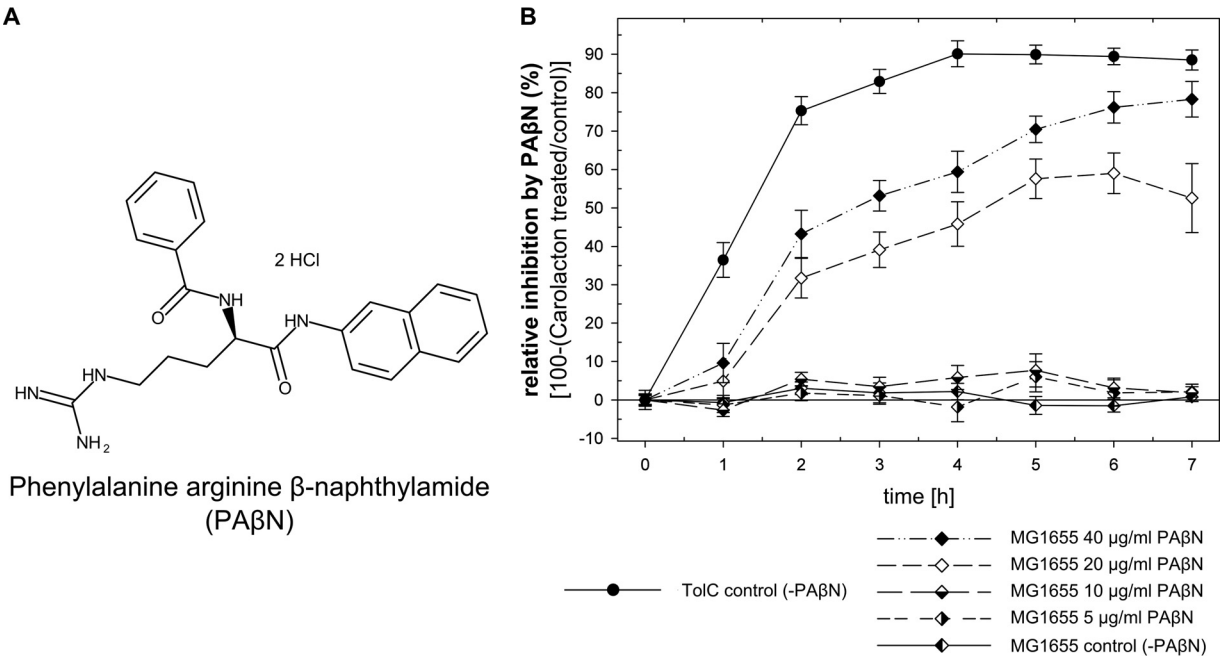

FIG 6 Inhibition of the AcrAB-TolC complex by PAβN leads to susceptibility of wild-type *E. coli* to carolacton. (A) Structure of the EPI PAβN. (B) Relative growth inhibition of *E. coli* TolC and *E. coli* K-12 MG1655 by carolacton in the presence of PAβN, as the percentage of control growth. The relative inhibition was calculated by dividing the OD of the carolacton-treated culture by the OD of the untreated control for every time point; both cultures contained the indicated amount of PAβN. Data show means and standard deviations for results from three biological replicates.

TABLE 2 MICs of carolacton against a *tolC*-complemented strain of *E. coli* TolC

Strain	MIC of carolacton (μg/ml)
E. coli TolC/pIB166-*tolC*	>8
E. coli TolC/pIB166-*tolC* (with 40 μg/ml PAβN)	2

sequence of the genetically uncharacterized, highly carolacton-susceptible *E. coli* TolC strain and revealed that it (i) shares the highest nucleotide sequence homology with *E. coli* MG1655 and (ii) is also phylogenetically reliably placed in a highly supported group that primarily harbors other K-12 strains. Originally, in the 1950s, the chromosome of the wild-type *E. coli* K-12 was cured from phage λ, generating *E. coli* K-12 W1485. *E. coli* K-12 W1485 was subsequently cured of its F^+ factor to make MG1655 (36). Thus, as *E. coli* TolC still contains the phage λ and a chromosomal copy of the F plasmid, our TolC strain appears to be an ancient prototrophic derivative of the original wild-type *E. coli* K-12. The profile of MIC resistance of *E. coli* TolC provided further evidence for an impairment of the efflux function in the mutant strain, rather than a change in the permeability of the outer membrane (25). As the biological function of the TolC OMP is of great scientific interest, *tolC* deletion mutants of *E. coli* are often generated anew, elaborately and with varied techniques for every study and in different, often-undescribed genetic backgrounds (25, 27, 28). The *E. coli* TolC strain sequenced here has now been thoroughly characterized. It is closely related to the ancestral *E. coli* wild-type strain K-12 and publicly available and thus could be used as a standard tool in the future.

A strong growth inhibition of *E. coli* TolC occurred at 0.25 μg/ml (0.54 μM). At this concentration, growth of *S. pneumoniae* TIGR4 is inhibited in a similar way, indicating a bacteriostatic role of carolacton (24). The same concentration of carolacton caused cell death in biofilms of *S. mutans* (20). A carolacton epimer, C-9 (*R*) (*epi*-carolacton), lacked biological activity in all organisms tested so far (22, 24). Here, we showed that it was also inactive when testing growth of the highly carolacton-sensitive *E. coli* TolC strain. The complete loss of biological activity of this carolacton derivative, with a mere inversion of a single stereogenic center at C-9, indicates a specific interaction of carolacton with a cellular target. A target that is present not only in streptococci (24) but also in Gram-negative bacteria like *Aggregatibacter* (22) and *E. coli*, and thus might be conserved in the phyla *Firmicutes* and *Proteobacteria*.

The data demonstrate that carolacton can enter the Gram-negative cell but is a substrate of the tripartite multidrug efflux pump AcrAB-TolC, the main component of intrinsic antibiotic resistance in *Enterobacteriaceae*. Its clinical application would therefore require high concentrations, or could be combined with efflux pump inhibitors. Treatment of the *E. coli* MG1655 with 40 μg/ml of PAβN, specific for inhibition of the AcrAB-TolC and AcrEF-TolC efflux complexes (16), rendered the strain susceptible to carolacton in a similar way as the deletion of TolC. The effect of AcrEF for the export of carolacton can be neglected here, as its expression is very low and this exporter has a

TABLE 3 Effect of carolacton treatment and PAβN on growth kinetics of the *E. coli* strains

E. coli strain and treatment[a]	Maximum specific growth rate (μ_{max}, h^{-1})		Doubling time (min)	
	Control	Carolacton[b]	Control	Carolacton[b]
MG1655	1.65 (±0.03)	1.67 (±0.05)	25.1 (±0.4)	25.0 (±0.7)
MG1655, 40 μg/ml PAβN	0.77 (±0.05)	**0.17 (±0.05)****	54.3 (±3.6)	**257.2 (±59)***
TolC	1.66 (±0.05)	**0.11 (±10^{-3})****	25.0 (±0.7)	**372.5 (±6)****
TolC, 40 μg/ml PAβN	0.82 (±0.05)	**0.05 (±10^{-3})****	51.0 (±2.9)	**899.5 (±44)****
TolC, *epi*-carolacton	1.68 (±0.01)	1.67 (±0.02)	24.7 (±0.2)	24.9 (±0.3)
TolC/pIB166-*tolC*	1.63 (±0.19)	1.54 (±0.2)	25.9 (±3.1)	27.4 (±3.5)
TolC/pIB166-*tolC*, 40 μg/ml PAβN	0.75 (±0.04)	**0.11 (±10^{-3})****	55.4 (±0.6)	451.9 (±190)

[a]Carolacton was applied at a final concentration of 0.25 μg/ml, except when *epi*-carolacton was used for treatment at the same final concentration.
[b]Values in boldface were significantly different from the control, based on a two-tailed Student's *t* test. **, $P \leq 0.001$; *, $P \leq 0.01$.

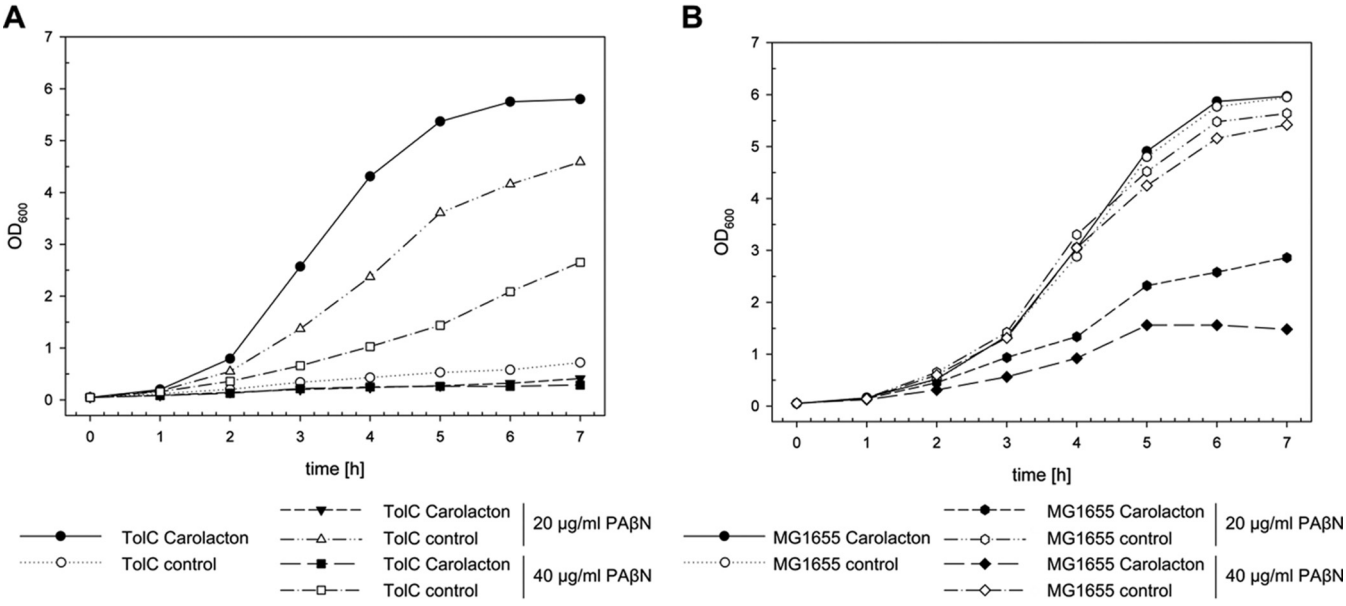

FIG 7 Effect of carolacton in combination with PAβN on growth of *E. coli* strains. (A) Growth inhibition of *E. coli* TolC by carolacton (circles), 20 μg/ml PAβN (triangles), or 40 μg/ml PAβN (squares). (B) Inhibition of *E. coli* K-12 MG1655 by carolacton (circles), 20 μg/ml PAβN (hexagons), or 40 μg/ml PAβN (diamonds). Carolacton was added in the experiments shown in panels A and B at a final concentration of 0.25 μg/ml where indicated. The figure is representative of the results of three independent biological replicates.

primary role in cell division (37); hence, deletion of *acrEF* does not change the antibiotic resistance phenotype of *E. coli* (11). Interestingly, lower concentrations of PAβN did not influence the sensitivity to carolacton at all, which is puzzling, because carolacton was provided at 0.25 μg/ml and inhibition by PAβN has been reported to be competitive (16).

The RNA-seq data for *E. coli* TolC indicated a strong regulatory response upon treatment with carolacton within the first 30 min, where growth is still unaffected, confirming the entry of carolacton into the cell and its likely immediate interaction with an intracellular target. The observed changes involved small regulatory RNAs, a sigma factor, chaperones, heat and cold shock proteins, flagellar components, and membrane transport proteins. The sigma factor F (σ^{28} in *E. coli*) is needed for flagellar assembly and motility (38), in accordance with the upregulation of the flagellar components *fliL* (*btd92_01821*) or *fliJ* (*btd92_01823*). Interestingly, all ncRNAs of the StyR-44 family were strongly upregulated already at the 5-min time point. Styr-44 ncRNAs are found in ribosomal operons located upstream of the 23S rRNA; their expression is dependent on the growth rate, but their specific function is unknown (39). As ncRNAs are known to act as global regulators of gene expression (40), their differential transcript abundance shows a fast and strong global regulatory response to carolacton. Carolacton treatment also caused upregulation of the outer membrane pore proteins NmpC ($\log_2$ FC, 2.72) and PhoE ($\log_2$ FC, 2.85), both of which play a role under heat shock and phosphorus starvation conditions, respectively (41, 42). The transcriptome data showed that the molecular target of carolacton may be located within a central metabolic pathway in the cell, and inhibition of this target induces multiple metabolic and transcriptional adaptations.

In conclusion, we found that carolacton efficiently penetrates the Gram-negative cell envelope, and low micromolar concentrations are sufficient for growth inhibition of *E. coli*, unless it is exported by the tripartite AcrAB-TolC efflux system. Carolacton might potentially be used against Gram-negative bacteria in combination with EPIs.

MATERIALS AND METHODS

Bacterial strains and growth conditions. *E. coli* strains used for growth experiments (Table 4) were routinely grown under aerobic conditions in Luria-Bertani (LB) broth overnight (o/n) at 37°C (200 rpm).

TABLE 4 *E. coli* strains and plasmids used in this study

Strain or plasmid	Relevant genotype or description	Reference or source
Strains		
DH5α	Cloning strain	Stratagene
K-12 MG1655	F^- λ^- Δ*ilvG rfb-50 rph-1*	DSM 18039
TolC	F^+ λ^+ Δ*ilvG rfb-50 ropS* (33Am) Δ*tolC*	Laboratory collection, DSM 104619
TolC/pIB166-*tolC*	TolC strain containing pIB166-*tolC* for complementation of strain TolC, Cm^r	This work
Plasmids		
pIB166	Cm^r	69
pIB166-*tolC*	Removal of P_{23} and integration of *tolC* under control of its native promoter (P_{tolC}-*tolC*), Cm^r	This work

The cultures were then used to inoculate fresh LB medium to an OD_{600} of 0.05, which was determined photospectrometrically (Ultrospec 3100 Pro; Amersham Biosciences, Inc.). Cultures with an OD_{600} of >0.5 were diluted in LB broth to below 0.5 in order to maintain the linearity between the measured absorbance and cell density and to achieve the most exact results. The initial culture was then split into equal volumes and supplemented with carolacton, 9(*R*) *epi*-carolacton, or PAβN, or maintained as untreated controls. For cryo-conservation, *E. coli* was grown in LB o/n, mixed with an equal volume of 50% (vol/vol) glycerol in cryovials, and frozen at −80°C.

Storage of carolacton, *epi*-carolacton, and PAβN. Carolacton and its derivative 9(*R*)-carolacton were dissolved in methanol or DMSO to a final concentration of 5.3 mM (250 μg/ml) or 2 mM (94.3 μg/ml), respectively, and stored in small aliquots in amber glass vials at −20°C in the dark. PAβN (25 mg/ml in H_2O) was stored at −20°C and used at final concentrations between 5 and 40 μg/ml, as indicated.

Complementation of *E. coli* TolC. Chemo-competent cells of *E. coli* were prepared according to the TSS method described by Chung et al. (43). pIB166 was PCR amplified with Phusion polymerase (NEB) using primers (pIB166_fwd and pIB166_rev), thereby eliminating P_{23} (Table 5). Genomic DNA of *E. coli* K-12 MG1655 served as a template for PCR amplification of the *tolC* locus (*b3035*), using primers (tolC_fwd and tolC_rev), additionally introducing flanks homologous to the linearized vector sequence. PCR products were purified with a PCR purification kit (Qiagen, Germany). The PCR-amplified *tolC* gene was cloned into pIB166 by using the CloneEZ kit (Genescript), and the reaction mix was transformed into *E. coli* DH5α. Obtained plasmids were verified by sequencing and subsequently transformed into *E. coli* TolC. *E. coli* transformed with pIB166 or its derivatives were grown on LB agar plates or in liquid LB broth containing 20 μg/ml chloramphenicol.

Determination of MIC values. MIC values of selected antibiotics and of carolacton against *E. coli* and *E. coli* K-12 MG1655 were determined by 2-fold serial microdilution in LB broth with incubation at 37°C for 20 h, as described previously (44). Antibiotics were tested in the following dilution ranges: ampicillin (32 to 0.25 μg/ml), carolacton (8 to 0.03 μg/ml), cephalotin (32 to 0.25 μg/ml), cefotaxime (1 to 0.078 μg/ml), cerulenin (32 to 0.25 μg/ml), ciprofloxacin (0.25 to 0.0019 μg/ml), chloramphenicol (64 to 0.5 μg/ml), corallopyronin A (32 to 0.25 μg/ml), erythromycin (64 to 0.5 μg/ml), gentamicin (32 to 0.25 μg/ml), kanamycin (8 to 0.03 μg/ml), novobiocin (16 to 0.125 μg/ml), penicillin G (32 to 0.25 μg/ml), phosphomycin (32 to 0.25 μg/ml), rifampin (32 to 0.25 μg/ml), sorangicin (32 to 0.25 μg/ml), sulfamethoxazole (256 to 2 μg/ml), triclosan (1 to 0.078 μg/ml), trimethoprim (2 to 0.015 μg/ml), and vancomycin (256 to 2 μg/ml), if not indicated otherwise. Corallopyronin A and sorangicin were kindly provided by Rolf Jansen (HZI, Braunschweig). Antibiotics were purchased from Sigma-Aldrich (Steinheim, Germany) or Carl Roth GmbH (Karlsruhe, Germany). MICs were the lowest concentrations that did not yield visible bacterial growth. The cell count of the initial inoculum was 5×10^5 CFU/ml, which was confirmed by plating of serial cell dilutions and counting of CFU. MICs were confirmed in at least two independent experiments.

Growth kinetics. The maximal specific growth rate (μ_{max}, per hour) and doubling time (t_D, in minutes) of bacteria were determined from semilogarithmically transformed growth curves (Fig. 8) according to methods described previously (45).

Extraction of genomic DNA and PacBio/Illumina sequencing. Genomic DNA of *E. coli* TolC was extracted by gravity flow using the Genomic-tip 20/G kit (Qiagen, Germany). Purified genomic DNA of *E. coli* TolC was processed for PacBio SMRT sequencing and Illumina MiSeq paired-end sequencing (2 ×

TABLE 5 Overview of oligonucleotides used

Primer	Sequence (5′–3′)	Purpose	Reference
pIB166_fwd	AATTCTAGAGCTCGAGATCTATCGATAAGC	Linearization of pIB166	This work
pIB166_fwd	CAGTCTTAGGTCTGATTTTTTATTTCTATTATTTAC		
tolC_fwd	ATCAGACCTAAGACTGAATGTCCTGGCACTAATAGTGAATTAAATGTGAATTTC	Cloning of *tolC* (*b3035*) of *E. coli* K-12 MG1655	This work
tolC_rev	CTCGAGCTCTAGAATTTCAGTTACGGAAAGGGTTATGACCGTTACTGGTGGT		

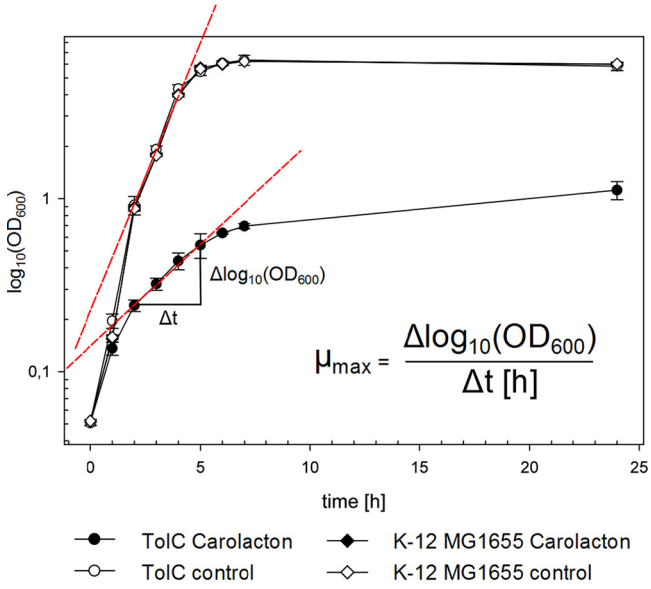

FIG 8 Example of the determination of the maximal specific growth rates of *E. coli* strains. The maximal specific growth rate (μ_{max}, per hour) was calculated from semilogarithmically transformed growth curves according to methods described previously (45).

250 bp) with a target genome coverage of 150-fold. DNA libraries for MiSeq sequencing of the genome of *E. coli* TolC were prepared with the NEBNext Ultra DNA library prep kit for Illumina sequencing (New England Biolabs, Ipswich, MA). Quality controls of NEBNext Ultra DNA libraries were conducted by fluorometric quantitation using the Qubit 3.0 fluorometer (Thermo, Fisher Scientific, Germany). For PacBio SMRT sequencing, a PacBio SMRTbell library was constructed according to the manufacturer's instructions and the library was sequenced on the PacBio RSII platform. *De novo* genome assemblies were built with PacBio's SMRT Portal (v.2.3.0) by utilizing the Hierarchical Genome Assembly Process 3 (HGAP3) (46). The genome was error corrected against indel errors by a mapping of Illumina reads onto finished genomes, using BWA (47) with subsequent variant and consensus calling using VarScan (48); automated sequence annotation was performed with Prokka (v.1.8) (49).

RNA isolation. Overnight cultures of *E. coli* TolC (OD_{600}, ~5) were diluted 1:200 in LB broth and grown to an OD_{600} of 0.1. The culture was subsequently divided into equal parts: one part was treated with 0.25 μg/ml carolacton, and the other part was treated with an equal volume of solvent (methanol). Cells were sampled before treatment and at 5, 15, and 30 min post-addition of carolacton. The samples were transferred to an equal volume of RNAProtect (Qiagen, Germany) and incubated for 5 min at room temperature. Cells were pelleted (13,000 rpm, 2 min), the supernatant was removed, and the pellet was frozen at −80°C. For RNA extraction, the pellets were washed with 0.5 ml nuclease-free water and centrifuged (13,000 rpm, 2 min). RNA extraction was carried out using the miRNeasy minikit (Qiagen, Germany) according to the manufacturer's instructions for purification of total RNA. The removal of genomic DNA was carried out by the optional on-column DNase I digestion using the DNase I kit (Qiagen, Germany) for 45 min. After the washing steps, the RNA was eluted in 50 μl of nuclease-free water supplied with the kit. To test the integrity of the isolated total RNA and the enriched mRNA, samples were analyzed using the Agilent 2100 Bioanalyzer and the RNA 6000 Pico kit (Agilent, Germany).

Enrichment of mRNA and RNA sequencing. mRNA enrichment was achieved by using the RiboZero kit for Gram-negative bacteria (epicenter; Illumina) for 2 μg of total RNA as described by the manufacturer. Successful removal of rRNA was verified using an Agilent 2100 Bioanalyzer (Agilent, Germany). Direct strand-specific RNA sequencing was performed using the Illumina HiSeq 2500 platform (Illumina) according to the ScriptSeq v.2 protocol for RNA-seq library construction (Agilent, Germany). After quality control and clipping of adapter sequences (primers and bar codes), mapping of reads and data analysis was conducted using the Rockhopper software (v.2.0.3) (50).

RNA-seq data analysis. Trimming of Illumina sequencing adapter sequences of obtained reads was achieved using fastq-mcf (51). Reads were mapped to the *E. coli* TolC genome (CP018801.1), and the read counts per feature were determined with Rockhopper (v.2.0.3) (50, 52). For analysis of differential abundance of transcripts, the raw read counts obtained with Rockhopper (53) were used, and changes in transcript abundance levels were calculated with the Bioconductor edgeR package (v.3.1) for R (v.3.10.0) (54, 55). False-discovery rate (FDR)-adjusted *P* values were calculated according to methods described previously (56). FDR values of <0.01 were considered significant. Heat maps were generated for genes that showed a $\log_2$ FC of $\geq \pm 2$ for at least one time point (FDR, ≤ 0.01), $\log_2$ FC values of transcript abundance obtained with edgeR were used as input for the heatmap.2 function of the R package gplots (v.2.15.0) (57).

Whole-genome-based phylogenomic analyses. To elucidate the phylogenetic positioning of strain TolC, and given its high sequence similarity to strain *E. coli* K-12 MG1655, a member of phylogroup A (58),

a corresponding reference data set was defined. The latter included all 32 members of phylogroup A, according to methods described previously (58), and was further complemented by four recently genome-sequenced strains that had been found to be highly similar to TolC (accession numbers NZ_CP011495, NZ_CP014225, NZ_CP014348, and NZ_CP016018). Two whole-genome-based phylogenomic analyses were conducted using the genome BLAST distance phylogeny approach (59) in its latest version (29). The first analysis was based on the nucleotide data restricted to genes, whereas the second one used protein data only. Coding regions were determined via Prodigal under default settings (60). All pairwise intergenomic distances were calculated with GBDP under established settings (58), i.e., using the trimming algorithm, distance formula d_5, and an E value cutoff of 10^{-8}. A total of 100 pseudobootstrap replicates were calculated per distance and later used for the inference of branch support values (61). Phylogenetic trees were inferred from the original and pseudobootstrapped distance matrices by using FastME 2.1.4 (62) under the SPR branch-swapping option and rooted using the midpoint method (63).

Software GBDP-based *in silico* DNA-DNA hybridization was achieved with the online version of the Genome-to-Genome Distance Calculator (GGDC v.2.1; http://ggdc.dsmz.de) (29), using the output of formula 2 (i.e., robust against the use of incomplete genome sequences), as recommended by the software creators. Whole-genome comparisons between *E. coli* strains were conducted with the BLAST Ring Image Generator (v.0.95) (64) and Easyfig (v.2.2.2) (65), both of which utilize BLAST+ (v.2.5.0) (66).

Accession number(s). The genome sequences of *E. coli* TolC were deposited in NCBI's GenBank (67) under accession number CP018801.1. Raw and processed RNA-seq data were deposited in NCBI's Gene Expression Omnibus (GEO) database (68) and are accessible through GEO Series accession number GSE93125.

SUPPLEMENTAL MATERIAL

Supplemental material for this article may be found at https://doi.org/10.1128/mSphereDirect.00375-17.

DATA SET S1, XLSX file, 0.5 MB.

DATA SET S2, XLSX file, 0.02 MB.

ACKNOWLEDGMENTS

We are thankful to Bettina Elxnat for excellent technical assistance. Furthermore, we thank Cathrin Spröer, Simone Severitt, and Nicole Heyer for PacBio DNA library construction and Isabel Schober for genome finishing. We are grateful to Rolf Jansen for providing sorangicin and corallopyronin, and we thank Mark Brönstrup for his suggestion to test the synergistic activity of carolacton with efflux pump inhibitors.

This work was carried out as an integral part of the BIOFABRICATION FOR NIFE Initiative, which is financially supported by the ministry of Lower Saxony and the Volkswagen Stiftung (NIFE is the Lower Saxony Center for Biomedical Engineering, Implant Research and Development, a joint translational research center of the Hannover Medical School, the Leibniz University Hannover, the University of Veterinary Medicine Hannover, and the Laser Center Hannover).

This work was funded by the German Ministry for Research and Technology (BMBF) in the program e:bio (grant number 031 A299) and by the President's Initiative and Networking Fund of the Helmholtz Association of German Research Centres (HGF) under contract number VH-GS-202.

We declare that the research was conducted in the absence of any commercial or financial relationships that could be construed as a potential conflict of interest.

REFERENCES

1. Silver LL. 2011. Challenges of antibacterial discovery. Clin Microbiol Rev 24:71–109. https://doi.org/10.1128/CMR.00030-10.
2. Silhavy TJ, Kahne D, Walker S. 2010. The bacterial cell envelope. Cold Spring Harb Perspect Biol 2:a000414. https://doi.org/10.1101/cshperspect.a000414.
3. Soto SM. 2013. Role of efflux pumps in the antibiotic resistance of bacteria embedded in a biofilm. Virulence 4:223–229. https://doi.org/10.4161/viru.23724.
4. Piddock LJV. 2006. Clinically relevant chromosomally encoded multidrug resistance efflux pumps in bacteria. Clin Microbiol Rev 19:382–402. https://doi.org/10.1128/CMR.19.2.382-402.2006.
5. Andersen JL, He GX, Kakarla P, Ranjana KC, Kumar S, Lakra WS, Mukherjee MM, Ranaweera I, Shrestha U, Tran T, Varela MF. 2015. Multidrug efflux pumps from *Enterobacteriaceae*, *Vibrio cholerae* and *Staphylococcus aureus* bacterial food pathogens. Int J Environ Res Publ Health 12:1487–1547. https://doi.org/10.3390/ijerph120201487.
6. Padilla E, Llobet E, Doménech-Sánchez A, Martínez-Martínez L, Bengoechea JA, Albertí S. 2010. *Klebsiella pneumoniae* AcrAB efflux pump contributes to antimicrobial resistance and virulence. Antimicrob Agents Chemother 54:177–183. https://doi.org/10.1128/AAC.00715-09.
7. Poole K. 2001. Multidrug efflux pumps and antimicrobial resistance in *Pseudomonas aeruginosa* and related organisms. J Mol Microbiol Biotechnol 3:255–264.
8. Nishino K, Latifi T, Groisman EA. 2006. Virulence and drug resistance roles of multidrug efflux systems of *Salmonella enterica* serovar Typhimurium. Mol Microbiol 59:126–141. https://doi.org/10.1111/j.1365-2958.2005.04940.x.
9. Daury L, Orange F, Taveau JC, Verchére A, Monlezun L, Gounou C, Marreddy RKR, Picard M, Broutin I, Pos KM, Lambert O. 2016. Tripartite

assembly of RND multidrug efflux pumps. Nat Commun 7:10731. https://doi.org/10.1038/ncomms10731.
10. Nikaido H, Takatsuka Y. 2009. Mechanisms of RND multidrug efflux pumps. Biochim Biophys Acta 1794:769–781. https://doi.org/10.1016/j.bbapap.2008.10.004.
11. Sulavik MC, Houseweart C, Cramer C, Jiwani N, Murgolo N, Greene J, DiDomenico B, Shaw KJ, Miller GH, Hare R, Shimer G. 2001. Antibiotic susceptibility profiles of Escherichia coli strains lacking multidrug efflux pump genes. Antimicrob Agents Chemother 45:1126–1136. https://doi.org/10.1128/AAC.45.4.1126-1136.2001.
12. Liu A, Tran L, Becket E, Lee K, Chinn L, Park E, Tran K, Miller JH. 2010. Antibiotic sensitivity profiles determined with an *Escherichia coli* gene knockout collection: generating an antibiotic bar code. Antimicrob Agents Chemother 54:1393–1403. https://doi.org/10.1128/AAC.00906-09.
13. Tegos GP, Haynes M, Strouse JJ, Khan MM, Bologa CG, Oprea TI, Sklar LA. 2011. Microbial efflux pump inhibition: tactics and strategies. Curr Pharm Des 17:1291–1302. https://doi.org/10.2174/138161211795703726.
14. Stavri M, Piddock LJV, Gibbons S. 2007. Bacterial efflux pump inhibitors from natural sources. J Antimicrob Chemother 59:1247–1260. https://doi.org/10.1093/jac/dkl460.
15. Renau TE, Léger R, Flamme EM, Sangalang J, She MW, Yen R, Gannon CL, Griffith D, Chamberland S, Lomovskaya O, Hecker SJ, Lee VJ, Ohta T, Nakayama K. 1999. Inhibitors of efflux pumps in *Pseudomonas aeruginosa* potentiate the activity of the fluoroquinolone antibacterial levofloxacin. J Med Chem 42:4928–4931. https://doi.org/10.1021/jm9904598.
16. Misra R, Morrison KD, Cho HJ, Khuu T. 2015. Importance of real-time assays to distinguish multidrug efflux pump-inhibiting and outer membrane-destabilizing activities in *Escherichia coli*. J Bacteriol 197:2479–2488. https://doi.org/10.1128/JB.02456-14.
17. Hsieh PC, Siegel SA, Rogers B, Davis D, Lewis K. 1998. Bacteria lacking a multidrug pump: a sensitive tool for drug discovery. Proc Natl Acad Sci U S A 95:6602–6606. https://doi.org/10.1073/pnas.95.12.6602.
18. Harvey AL, Edrada-Ebel R, Quinn RJ. 2015. The re-emergence of natural products for drug discovery in the genomics era. Nat Rev Drug Discov 14:111–129. https://doi.org/10.1038/nrd4510.
19. Jansen R, Irschik H, Huch V, Schummer D, Steinmetz H, Bock M, Schmidt T, Kirschning A, Müller R. 2010. Carolacton: a macrolide ketocarbonic acid that reduces biofilm formation by the caries- and endocarditis-associated bacterium *Streptococcus mutans*. Eur J Org Chem 2010:1284–1289. https://doi.org/10.1002/ejoc.200901126.
20. Kunze B, Reck M, Dötsch A, Lemme A, Schummer D, Irschik H, Steinmetz H, Wagner-Döbler I. 2010. Damage of *Streptococcus mutans* biofilms by carolacton, a secondary metabolite from the myxobacterium *Sorangium cellulosum*. BMC Microbiol 10:199. https://doi.org/10.1186/1471-2180-10-199.
21. Reck M, Rutz K, Kunze B, Tomasch J, Surapaneni SK, Schulz S, Wagner-Döbler I. 2011. The biofilm inhibitor carolacton disturbs membrane integrity and cell division of *Streptococcus mutans* through the serine/threonine protein kinase PknB. J Bacteriol 193:5692–5706. https://doi.org/10.1128/JB.05424-11.
22. Stumpp N, Premnath P, Schmidt T, Ammermann J, Dräger G, Reck M, Jansen R, Stiesch M, Wagner-Döbler I, Kirschning A. 2015. Synthesis of new carolacton derivatives and their activity against biofilms of oral bacteria. Org Biomol Chem 13:5765–5774. https://doi.org/10.1039/C5OB00460H.
23. Reck M, Wagner-Döbler I. 2016. Carolacton treatment causes delocalization of the cell division proteins PknB and DivIVa in *Streptococcus mutans* in vivo. Front Microbiol 7:684. https://doi.org/10.3389/fmicb.2016.00684.
24. Donner J, Reck M, Bergmann S, Kirschning A, Müller R, Wagner-Döbler I. 2016. The biofilm inhibitor carolacton inhibits planktonic growth of virulent pneumococci via a conserved target. Sci Rep 6:29677. https://doi.org/10.1038/srep29677.
25. Augustus AM, Celaya T, Husain F, Humbard M, Misra R. 2004. Antibiotic-sensitive TolC mutants and their suppressors. J Bacteriol 186:1851–1860. https://doi.org/10.1128/JB.186.6.1851-1860.2004.
26. Freddolino PL, Amini S, Tavazoie S. 2012. Newly identified genetic variations in common *Escherichia coli* MG1655 stock cultures. J Bacteriol 194:303–306. https://doi.org/10.1128/JB.06087-11.
27. Bleuel C, Grosse C, Taudte N, Scherer J, Wesenberg D, Krauss GJ, Nies DH, Grass G. 2005. TolC is involved in enterobactin efflux across the outer membrane of *Escherichia coli*. J Bacteriol 187:6701–6707. https://doi.org/10.1128/JB.187.19.6701-6707.2005.
28. Deininger KNW, Horikawa A, Kitko RD, Tatsumi R, Rosner JL, Wachi M, Slonczewski JL. 2011. A requirement of TolC and MDR efflux pumps for acid adaptation and GadAB induction in *Escherichia coli*. PLoS One 6:e18960. https://doi.org/10.1371/journal.pone.0018960.
29. Meier-Kolthoff JP, Auch AF, Klenk HP, Göker M. 2013. Genome sequence-based species delimitation with confidence intervals and improved distance functions. BMC Bioinformatics 14:60. https://doi.org/10.1186/1471-2105-14-60.
30. Lawther RP, Calhoun DH, Adams CW, Hauser CA, Gray J, Hatfield GW. 1981. Molecular basis of valine resistance in *Escherichia coli* K-12. Proc Natl Acad Sci U S A 78:922–925. https://doi.org/10.1073/pnas.78.2.922.
31. Kuhnert P, Nicolet J, Frey J. 1995. Rapid and accurate identification of *Escherichia coli* K-12 strains. Appl Environ Microbiol 61:4135–4139. https://doi.org/10.7892/boris.62554.
32. Rak B, von Reutern M. 1984. Insertion element IS*5* contains a third gene. EMBO J 3:807–811.
33. Rak B, Lusky M, Hable M. 1982. Expression of two proteins from overlapping and oppositely oriented genes on transposable DNA insertion element IS*5*. Nature 297:124–128. https://doi.org/10.1038/297124a0.
34. Irschik H, Jansen R, Höfle G, Gerth K, Reichenbach H. 1985. The corallopyronins, new inhibitors of bacterial RNA synthesis from myxobacteria. J Antibiot 38:145–152. https://doi.org/10.7164/antibiotics.38.145.
35. Irschik H, Jansen R, Gerth K, Höfle G, Reichenbach H. 1987. The sorangicins, novel and powerful inhibitors of eubacterial RNA polymerase isolated from myxobacteria. J Antibiot 40:7–13. https://doi.org/10.7164/antibiotics.40.7.
36. Hayashi K, Morooka N, Yamamoto Y, Fujita K, Isono K, Choi S, Ohtsubo E, Baba T, Wanner BL, Mori H, Horiuchi T. 2006. Highly accurate genome sequences of *Escherichia coli* K-12 strains MG1655 and W3110. Mol Syst Biol 2:2006.0007. https://doi.org/10.1038/msb4100049.
37. Lau SY, Zgurskaya HI. 2005. Cell division defects in *Escherichia coli* deficient in the multidrug efflux transporter AcrEF-TolC. J Bacteriol 187:7815–7825. https://doi.org/10.1128/JB.187.22.7815-7825.2005.
38. Treviño-Quintanilla LG, Freyre-González JA, Martínez-Flores I. 2013. Anti-sigma factors in E. coli: common regulatory mechanisms controlling sigma factors availability. Curr Genomics 14:378–387. https://doi.org/10.2174/1389202911314060007.
39. Chinni SV, Raabe CA, Zakaria R, Randau G, Hoe CH, Zemann A, Brosius J, Tang TH, Rozhdestvensky TS. 2010. Experimental identification and characterization of 97 novel npcRNA candidates in Salmonella enterica serovar Typhi. Nucleic Acids Res 38:5893–5908. https://doi.org/10.1093/nar/gkq281.
40. Waters LS, Storz G. 2009. Regulatory RNAs in bacteria. Cell 136:615–628. https://doi.org/10.1016/j.cell.2009.01.043.
41. Ruan L, Pleitner A, Gänzle MG, McMullen LM. 2011. Solute transport proteins and the outer membrane protein NmpC contribute to heat resistance of *Escherichia coli* AW1.7. Appl Environ Microbiol 77:2961–2967. https://doi.org/10.1128/AEM.01930-10.
42. Korteland J, Tommassen J, Lugtenberg B. 1982. PhoE protein pore of the outer membrane of *Escherichia coli* K12 is a particularly efficient channel for organic and inorganic phosphate. Biochim Biophys Acta 690:282–289. https://doi.org/10.1016/0005-2736(82)90332-7.
43. Chung CT, Niemela SL, Miller RH. 1989. One-step preparation of competent *Escherichia coli*: transformation and storage of bacterial cells in the same solution. Proc Natl Acad Sci U S A 86:2172–2175. https://doi.org/10.1073/pnas.86.7.2172.
44. Andrews JM. 2001. Determination of minimum inhibitory concentrations. J Antimicrob Chemother 48:5–16. https://doi.org/10.1093/jac/48.suppl_1.5.
45. Perni S, Andrew PW, Shama G. 2005. Estimating the maximum growth rate from microbial growth curves: definition is everything. Food Microbiol 22:491–495. https://doi.org/10.1016/j.fm.2004.11.014.
46. Chin CS, Alexander DH, Marks P, Klammer AA, Drake J, Heiner C, Clum A, Copeland A, Huddleston J, Eichler EE, Turner SW, Korlach J. 2013. Nonhybrid, finished microbial genome assemblies from long-read SMRT sequencing data. Nat Methods 10:563–569. https://doi.org/10.1038/nmeth.2474.
47. Li H, Durbin R. 2009. Fast and accurate short read alignment with Burrows-Wheeler transform. Bioinformatics 25:1754–1760. https://doi.org/10.1093/bioinformatics/btp324.
48. Koboldt DC, Zhang Q, Larson DE, Shen D, McLellan MD, Lin L, Miller CA, Mardis ER, Ding L, Wilson RK. 2012. VarScan 2: somatic mutation and copy number alteration discovery in cancer by exome sequencing. Genome Res 22:568–576. https://doi.org/10.1101/gr.129684.111.
49. Seemann T. 2014. Prokka: rapid prokaryotic genome annotation. Bioinformatics 30:2068–2069. https://doi.org/10.1093/bioinformatics/btu153.

50. Tjaden B. 2015. De novo assembly of bacterial transcriptomes from RNA-seq data. Genome Biol 16:1. https://doi.org/10.1186/s13059-014-0572-2.
51. Aronesty E. 2013. Comparison of sequencing utility programs. Open Bioinforma J 7:1–8. https://doi.org/10.2174/1875036201307010001.
52. McClure R, Balasubramanian D, Sun Y, Bobrovskyy M, Sumby P, Genco CA, Vanderpool CK, Tjaden B. 2013. Computational analysis of bacterial RNA-Seq data. Nucleic Acids Res 41:e140. https://doi.org/10.1093/nar/gkt444.
53. Anders S, McCarthy DJ, Chen Y, Okoniewski M, Smyth GK, Huber W, Robinson MD. 2013. Count-based differential expression analysis of RNA sequencing data using R and Bioconductor. Nat Protoc 8:1765–1786. https://doi.org/10.1038/nprot.2013.099.
54. Robinson MD, McCarthy DJ, Smyth GK. 2010. edgeR: a Bioconductor package for differential expression analysis of digital gene expression data. Bioinformatics 26:139–140. https://doi.org/10.1093/bioinformatics/btp616.
55. McCarthy DJ, Chen Y, Smyth GK. 2012. Differential expression analysis of multifactor RNA-Seq experiments with respect to biological variation. Nucleic Acids Res 40:4288–4297. https://doi.org/10.1093/nar/gks042.
56. Benjamini Y, Hochberg Y. 1995. Controlling the false discovery rate: a practical and powerful approach to multiple testing. J R Stat Soc B Stat Methodol 57:289–300.
57. Warnes GR, Bolker B, Bonebakker L, Gentleman R, Huber W, Liaw A, Lumley T, Maechler M, Magnusson A, Moeller S. 2013. Gplots: various R programming tools for plotting data. R package version 2.12.1. http://CRAN.R-project.org/package=gplots.
58. Meier-Kolthoff JP, Hahnke RL, Petersen J, Scheuner C, Michael V, Fiebig A, Rohde C, Rohde M, Fartmann B, Goodwin LA, Chertkov O, Reddy T, Pati A, Ivanova NN, Markowitz V, Kyrpides NC, Woyke T, Göker M, Klenk HP. 2014. Complete genome sequence of DSM 30083^T, the type strain (U5/41^T) of *Escherichia coli*, and a proposal for delineating subspecies in microbial taxonomy. Stand Genomic Sci 9:2. https://doi.org/10.1186/1944-3277-9-2.
59. Henz SR, Huson DH, Auch AF, Nieselt-Struwe K, Schuster SC. 2005. Whole-genome prokaryotic phylogeny. Bioinformatics 21:2329–2335. https://doi.org/10.1093/bioinformatics/bth324.
60. Hyatt D, Chen GL, Locascio PF, Land ML, Larimer FW, Hauser LJ. 2010. Prodigal: prokaryotic gene recognition and translation initiation site identification. BMC Bioinformatics 11:119. https://doi.org/10.1186/1471-2105-11-119.
61. Meier-Kolthoff JP, Auch AF, Klenk H-P, Göker M. 2014. Highly parallelized inference of large genome-based phylogenies. Concurr Comput 26:1715–1729. https://doi.org/10.1002/cpe.3112.
62. Lefort V, Desper R, Gascuel O. 2015. FastME 2.0: a comprehensive, accurate, and fast distance-based phylogeny inference program. Mol Biol Evol 32:2798–2800. https://doi.org/10.1093/molbev/msv150.
63. Farris JS. 1972. Estimating phylogenetic trees from distance matrices. Am Nat 106:645–668. https://doi.org/10.1086/282802.
64. Alikhan NF, Petty NK, Ben Zakour NL, Beatson SA. 2011. BLAST Ring Image Generator (Brig): simple prokaryote genome comparisons. BMC Genomics 12:402. https://doi.org/10.1186/1471-2164-12-402.
65. Sullivan MJ, Petty NK, Beatson SA. 2011. Easyfig: a genome comparison visualizer. Bioinformatics 27:1009–1010. https://doi.org/10.1093/bioinformatics/btr039.
66. Camacho C, Coulouris G, Avagyan V, Ma N, Papadopoulos J, Bealer K, Madden TL. 2009. Blast+: architecture and applications. BMC Bioinformatics 10:421. https://doi.org/10.1186/1471-2105-10-421.
67. Benson DA, Karsch-Mizrachi I, Lipman DJ, Ostell J, Wheeler DL. 2005. GenBank. Nucleic Acids Res 33:D34–D38. https://doi.org/10.1093/nar/gki063.
68. Barrett T, Wilhite SE, Ledoux P, Evangelista C, Kim IF, Tomashevsky M, Marshall KA, Phillippy KH, Sherman PM, Holko M, Yefanov A, Lee H, Zhang N, Robertson CL, Serova N, Davis S, Soboleva A. 2013. NCBI GEO: archive for functional genomics data sets: update. Nucleic Acids Res 41:D991–D995. https://doi.org/10.1093/nar/gks1193.
69. Biswas I, Jha JK, Fromm N. 2008. Shuttle expression plasmids for genetic studies in *Streptococcus mutans*. Microbiology 154:2275–2282. https://doi.org/10.1099/mic.0.2008/019265-0.